Altered glutamate signaling in Parkinson's disease patients with REM sleep behavior disorder

Christopher E.J. Doppler[1,2,*], Aline Seger[1,2,*], Ezequiel Farrher[3], Cláudia Régio Brambilla[3], Lukas Hensel[1,2], Christian P. Filss[4], Ana Gogishvili[3,5,6], N. Jon Shah[3,7,8,9], Christoph W. Lerche[3], Bernd Neumaier[10], Karl-Josef Langen[3,4], Gereon R. Fink[1,2], and Michael Sommerauer[1,2]

*shared first authorship

[1]Cognitive Neuroscience, Institute of Neuroscience and Medicine (INM-3), Forschungszentrum Jülich, 52425 Jülich, Germany

[2]University of Cologne, Faculty of Medicine and University Hospital Cologne, Department of Neurology, 50937 Köln, Germany

[3]Institute of Neuroscience and Medicine (INM-4), Forschungszentrum Jülich, 52425 Jülich, Germany

[4]Department of Nuclear Medicine, RWTH University Hospital, 52074 Aachen, Germany

[5]Faculty of Medicine, RWTH Aachen University, 52056 Aachen, Germany

[6]Engineering Physics Department, Georgian Technical University, Tbilisi, Georgia

[7]Institute of Neuroscience and Medicine (INM-11), Molecular Neuroscience and Neuroimaging, JARA, Forschungszentrum Jülich, 52425 Jülich, Germany

[8]JARA – BRAIN - Translational Medicine, 52056 Aachen, Germany

[9]Department of Neurology, RWTH Aachen University, 52056 Aachen, Germany

[10]Institute of Neuroscience and Medicine (INM-5), Forschungszentrum Jülich, 52425 Jülich, Germany

Abstract

Background and Objectives: Clinical heterogeneity of patients with Parkinson's disease is well recognized. Parkinson's disease with rapid eye movement (REM) sleep behavior disorder (RBD) is a more malignant phenotype with faster motor progression and higher non-motor symptom burden. However, the neural mechanisms underlying this clinical divergence concerning disbalances in neurotransmitter systems remain elusive.

Methods: Combining magnetic resonance (MR) spectroscopy and ^{11}C-ABP688 positron emission tomography (PET) on PET/MR hybrid system, we simultaneously investigated two different mechanisms of glutamate signaling in patients with Parkinson's disease. Thirty-three patients were grouped according to their RBD status in overnight video-polysomnography and compared to 15 age- and sex-matched healthy control (HC) subjects. Total volumes of distribution (V_T) of ^{11}C-ABP688 were estimated with metabolite-corrected plasma concentrations during steady-state conditions between minutes 45 to 60 of the scan following a bolus-infusion protocol. Glutamate, glutamine, and glutathione levels were investigated with single voxel STEAM MR spectroscopy of the left putamen.

Results: We measured globally elevated V_T of ^{11}C-ABP688 in patients with Parkinson's disease and RBD compared to patients without RBD and HC subjects ($F(2,45) = 5.579$, $p = 0.007$). Conversely, glutamatergic metabolites did not differ between groups and did not correlate with the regional V_T of ^{11}C-ABP688. V_T of ^{11}C-ABP688 correlated with the amount of REM sleep without atonia ($F(1,42) = 5.600$, $p = 0.023$), and with dopaminergic treatment response in Parkinson's disease patients ($F(1,30) = 5.823$, $p = 0.022$).

Conclusion: Our results suggest that patients with Parkinson's disease and RBD exhibit altered glutamatergic signaling indicated by higher V_T of ^{11}C-ABP688 despite unaffected glutamate metabolism. The disbalance of glutamate receptors and neurotransmitter might indicate a novel mechanism contributing to the heterogeneity of Parkinson's disease and warrants further investigation of drugs targeting mGluR5.

Introduction

Even though clinical diagnostic criteria of Parkinson's disease are mainly focused on extrapyramidal motor impairment, considered to be primarily driven by dopaminergic depletion of the basal ganglia,[1] clinical heterogeneity of the disease is well recognized.[2,3] This resonates well with multiple neurotransmitters beyond the dopaminergic system being affected by misfolded α-synuclein, potentially implying differential neurotransmitter pathology in PD subtypes.[4,5]

Parkinson's disease with rapid eye movement (REM) sleep behavior disorder (RBD) – a parasomnia characterized by insufficient muscle atonia and dream enacting behavior – is reported to exhibit a more malignant phenotype with faster motor progression and a higher burden of non-motor symptoms.[6,7] Using positron emission tomography (PET), profuse demise of the noradrenergic and cholinergic systems could be detected in Parkinson's disease patients with RBD, which was linked to cognitive deficits.[8,9]

Besides deficiencies of neurotransmitters caused by neurodegeneration, differences in the regulation of receptor expression and neurotransmitter metabolism might influence symptom prevalence as proposed for the evolvement of dyskinesias in Parkinson's disease.[10] Such receptor-neurotransmitter dysbalance might be particularly relevant for glutamate and its receptors, the brain's primary excitatory neurotransmitter involved in many physiological processes.[11–14] Although it has been suggested that glutamate is involved in the pathophysiology of RBD,[15] its contribution to the clinical phenotype of PD with RBD remains unclear. In addition to ionotropic glutamate receptors (including N-Methyl-d-Aspartate (NMDA), α-Amino-3-hydroxy-5-methyl-4-isoxazolepropionic Acid (AMPA) and kainate receptors), G protein-coupled metabotropic glutamate receptors (mGluR) are paramount for the regulation of glutamate signaling, particularly in the motor circuitry of the basal ganglia.[16] Specifically, inhibition of mGluR5 can ameliorate motor symptoms and even reduce dopaminergic and noradrenergic degeneration in Parkinson's disease animal models.[17,18] Conversely, activation of mGluR5 can lead to amplified neurodegeneration and might reinforce excitotoxicity.[19,20]

Taking together the malignant phenotype of RBD in Parkinson's disease and the distinctive role of mGluR5 in the basal ganglia motor circuitry and neurodegenerative processes, we aimed to elucidate the relationship between RBD and mGluR5 dysregulation. Using hybrid PET and magnetic resonance (MR) imaging and spectroscopy, we simultaneously examined glutamate

metabolite levels and V_T of ^{11}C-ABP688, a tracer with highly specific binding to the mGluR5, in Parkinson's disease patients with RBD and compared findings to patients without RBD and healthy control (HC) subjects.

Materials and methods

Participants

We recruited 33 patients with Parkinson's disease, diagnosed according to the current Movement Disorder Society (MDS) clinical diagnostic criteria,[1] from the tertiary Movement Disorders clinics at the University Hospital Cologne and advertisements in the patients' magazine of the German Parkinson's disease association. Twenty-six patients met the criteria for clinically established and seven for probable Parkinson's disease.[1] We additionally enrolled 15 HC subjects with no history of movement or psychiatric disorder from newspaper advertisements. Inclusion criteria were age between 51 and 80 years, geriatric depression scale (GDS 15) < 5, and Montreal cognitive assessment (MoCA) score > 22. Exclusion criteria encompassed contraindications for magnetic resonance (MR) imaging or positron emission tomography (PET), known sleep-related breathing disorder, active or former (less than 10 years cessation) smoking as this potentially influences ^{11}C-ABP688 binding,[21] and for Parkinson's disease patients a disease duration > 15 years. Medication influencing glutamatergic metabolism or signaling (e.g., amantadine and safinamide) had to be stopped five times its individual half-life before MR and PET scanning.

Clinical assessments

We recorded medical history and current medication in all subjects. Olfactory function was tested with Sniffin' Sticks, including 12 different odors. Autonomic symptoms were assessed with the scales for outcomes in Parkinson's disease - autonomic dysfunction (SCOPA-AUT), subjective sleeping quality with the Parkinson's disease sleep scale (PDSS), and symptoms of RBD with the REM sleep behavior disorder screening questionnaire (RBDSQ). We assessed motor symptom burden using the MDS Unified Parkinson's Disease Rating Scale III (MDS-UPDRS III) during regular ON state and OFF state 12 hours after discontinuation of dopaminergic medication in patients with Parkinson's disease. We calculated dopaminergic treatment response as the ratio of the MDS-UPDRS III score during ON state to the score during OFF state. Additionally, we recorded motor symptom duration, Hoehn and Yahr stage, and dopaminergic treatment as levodopa equivalent daily doses (LEDD) according to previously published conversion factors.[22]

Video-polysomnography

We used a mobile SOMNOscreen^{TM} plus device for overnight video-polysomnography. This device enables 10 EEG recordings (according to the international 10/20 system: F3, F4, C3, C4, O1, O2, A1, A2, Fpz as grounding, and Cz as reference), electrooculography, surface electromyography of the submental muscle and the tibialis anterior muscles, electrocardiography, nasal pressure and thermal flow monitoring, thoracic and abdominal respiratory effort belts, finger pulse oximetry, and synchronized audio-visual recording. Visual PSG scoring was performed by MS, who is a board-certified sleep expert, on 30-second epochs, including total sleep time, sleep efficiency, the absolute amount of stage 1 (N1), stage 2 (N2), slow wave sleep (SWS), and REM sleep, apnea-hypopnea index (AHI, number of apnea plus hypopnea events per hour of sleep), and periodic limb movements in sleep index (PLMSI, number of periodic leg movements per hour of sleep) according to the American Academy of Sleep (AASM) Manual for the Scoring of Sleep and Associated Events Version 2.6.[23]

Diagnosis of RBD was made blinded to clinical and imaging results according to AASM standards by consensus of MS and CD, fellow in sleep medicine for multiple years.[23] Furthermore, REM sleep without atonia (RSWA) was quantified as the percentage of REM sleep with increased muscle activity of the submental muscle according to the SINBAR criteria using *RBDtector* software (https://github.com/aroethen/RBDtector).[24] In brief, 'tonic activity' was defined as muscle activity persisting > 15s during a 30s REM epoch. 'Phasic activity' was scored as brief muscle activity > 0.2s but shorter than 5s, determined considering 3s REM mini epochs. 'Any activity' - as the most global measure of RSWA - included 'tonic' plus 'phasic activity' and muscle activity between 5s - 15s.[24] All activities are expressed as the percentage of REM sleep affected by RSWA.

^{11}C-ABP688 PET

Radiosynthesis of ^{11}C-ABP688 was performed as previously reported.[25] All subjects were measured using a Siemens Trio 3T MR scanner with a customized BrainPET insert.[26] Patients were scanned during a stable ON condition. The average total injected activity per subject was 589.4 ± 25.8 MBq ^{11}C-ABP688. Similar to a previous publication,[27] we applied 50% (range 47.9 - 55.8%) of total activity as a bolus, followed by a 65 min continuous infusion of the

remaining 50% (range 44.2 - 52.1%), providing steady-state conditions at 45 - 60 min after bolus injection (Supplementary Figure 1). PET data were acquired in list mode for 65 min and corrected for attenuation using an in-house template,[28] random and scattered coincidences, decay, and dead time. Image reconstruction was performed using 3D□OP□OSEM (2 subsets, 32 iterations), resulting in isotropic voxels of 1.25□mm³. We chose a frame scheme with increasing frame duration, including three 5 min frames between 45 - 60 min (Supplementary Figure 1).

We used PMOD 4.0 software and its relevant toolboxes for image analysis. First, dynamic PET images were motion corrected using an averaged image from 5 - 10 min post bolus injection as a template for rigid co-registration. Motion-corrected PET images were rigidly co-aligned to the corresponding anatomical T1-weighted MPRAGE images (TE 2.89 ms, TR 2500 ms, 1 mm³ isotropic voxels). Using MR-based segmentation, MR and PET images were normalized to Montreal Neurological Institute (MNI) space to delineate volumes of interest (VOIs) from the built-in Hammers atlas using the PNEURO tool. VOI delineations were manually corrected if necessary, and ^{11}C-ABP688 time activity curves from all VOIs were extracted. Bilateral VOIs of the following 13 brain regions were used for further analysis: frontal cortex, temporal cortex, parietal cortex, occipital cortex, insula, anterior cingulate, posterior cingulate, amygdala, hippocampus, caudate, putamen, pallidum, and thalamus. Ascertaining steady-state conditions between 45 - 60 minutes post bolus injection visually (Supplementary Figure 1) and by low coefficients of variance (mean, 1.0 ± 0.6%), we averaged ^{11}C-ABP688 concentrations from each VOI during that time.

We also took four plasma samples at 45, 50, 55, and 60 min after bolus injection. In order to obtain metabolite-corrected plasma concentrations, the parent compound was separated from the metabolites in each sample by solid-phase extraction using appropriate cartridges (Waters Sep-Pak® tC18) as previously described.[29] Again, steady-state conditions of plasma activities during 45 - 60 min post bolus injection were ascertained visually and by a low coefficient of variance (mean, 4.8 ± 2.5%), and we averaged all four metabolite-corrected plasma concentrations. We calculated regional brain V_T as follows: The radioligand concentration in the VOI (mean of 45 - 60 min) divided by metabolite-corrected plasma concentration (mean of 45 - 60 min).[30] Even though total injected activities ($H(2) = 0.405$, $p = 0.817$), plasma concentrations ($F(2) = 3.193$, $p = 0.050$), and parent compounds ($F(2) = 1.183$, $p = 0.316$) did not differ between groups, metabolite-corrected plasma concentrations differed significantly ($F(2) = 3.797$, $p = 0.030$): HC

subjects, 4.1 ± 0.9 kBq/ml, Parkinson's disease without RBD, 3.5 ± 0.8 kBq/ml, and Parkinson's disease with RBD, 3.3 ± 1.0 kBq/ml. We, therefore, included metabolite-corrected plasma concentrations as a covariate in our statistical model.

MR spectroscopy

During PET recording, we simultaneously acquired MR spectroscopy using a single voxel stimulated echo acquisition mode (STEAM) sequence[31] with the following parameters: echo time (TE) = 6 ms, repetition time (TR) = 4800 ms, mixing time (TM) 47.82 ms, 128 averages, receive-bandwidth = 2000 Hz. Before the acquisition, the radiofrequency power was calibrated for each subject, and B_0 shim was performed using FASTESTMAP.[32] The voxel was centered in the left putamen (voxel size: 21 (left-right) × 35 (anterior-posterior) × 21 (rostral-caudal) mm) (Supplementary Figure 2). One extra complete phase cycle was measured without water suppression for eddy-current correction and absolute quantification. All data were preprocessed utilizing the FID-A package in MATLAB 2015a, including removal of motion corrupted scans and phase as well as frequency drift correction.[33] The metabolite basis set used for quantification in LCModel (6.3-0I) was generated with VeSPA (https://scion.duhs.duke.edu/vespa/)[34] using previously published chemical shift and J-coupling constants,[35] including alanine, ascorbate, aspartate, creatine, γ-aminobutyric acid, glucose, glutamine, glutamate, glutathione, glycerophosphorylcholine, myo-inositol, lactate, n-acetylaspartate, n-acetylaspartylglutamate, phosphocreatine, phosphorylcholine, phosphorylethanolamine, scyllo-inositol, and taurine (Supplementary Figure 2). An additional macromolecular spectrum measured using STEAM at 3T obtained from the MM Consensus Data Collection repository (https://mrshub.org/datasets_mm) was also included in the metabolites basis set. For statistical analysis, we only considered the glutamatergic metabolites - glutamate, glutamine, and glutathione - as metabolites of interest in the context of mGluR5 availability.

The anatomical images were segmented using FAST[36] for cortical grey matter, white matter, and cerebrospinal fluid, and FIRST[37] for subcortical structures (FMRIB Software Library v6.0.3); the relative amounts within the MR spectroscopy voxel were determined. Metabolite concentrations were corrected for CSF content within the MRS voxel by dividing the concentration value obtained with LCModel by '1-CSF fraction'.

Acquisition of MRS failed in three subjects (one subject from each group) due to technical reasons. We additionally excluded three HC subjects, three Parkinson's disease patients without RBD, and four Parkinson's disease patients with RBD due to low spectral quality (full-width at half maximum > 0.07 ppm and signal-to-noise ratio < 20).

Statistical analysis

Data analysis was performed using the Statistical Package for the Social Sciences (SPSS) version 28. Group data are presented as mean ± standard deviation or relative frequencies unless otherwise stated. Normal data distribution was assessed with the Shapiro-Wilk test, Q-Q plots, and box plots. Group comparisons were calculated using Student's *t*, Mann-Whitney U, and chi-square tests, univariate analyses of variance (ANOVA), analyses of covariance (ANCOVA), and Kruskal-Wallis tests as appropriate. Correlation analyses were calculated using Spearman's *rho* and Pearson's *r*, according to the data distribution. VOI-based V_T of ^{11}C-ABP688 were compared using a repeated measures ANOVA with brain region (n = 13) as within-subject factor and group (n = 3) as between-subject factor. Post-hoc tests were applied to analyze differences in individual brain regions between the three groups. Significance was accepted at $p < 0.05$ uncorrected.

Standard Protocol Approvals, Registrations, and Patient Consents

The study was approved by the local ethics committee, and written informed consent was obtained from all study participants following the Declaration of Helsinki. Permission to use 11C-ABP688 was obtained from the federal office of radiation safety before the start of the study.

Data availability

Anonymized data are available upon reasonable request.

Results

Clinical assessments

HC subjects (n = 15), patients with Parkinson's disease without RBD (n = 17), and patients with RBD (n = 16) were comparable in age, sex, cognition, and depressive symptoms (Table 1). Patients with Parkinson's disease showed reduced olfactory discrimination and reported more autonomic symptoms and a higher burden of sleep disturbances (Table 1). Patients with Parkinson's disease without RBD and patients with RBD did not differ significantly regarding these non-motor symptoms as well as in clinical metrics of disease burden (e.g., motor symptom duration, motor deficits, and dopaminergic treatment doses, Table 1). Patients with RBD exhibited higher RBDSQ scores than HC subjects and patients without RBD (Table 1).

Similarly, polysomnographic metrics of sleep macroarchitecture did not differ between groups, but patients with Parkinson's disease with RBD exhibited significantly increased tonic, phasic, and any muscle activity during REM sleep compared to patients without RBD and HC subjects (Table 2).

^{11}C-ABP688 PET and glutamate MR spectroscopy

Repeated measures ANOVA across all three groups revealed significant differences of ^{11}C-ABP688 V_T ($F(2,45) = 5.579$, $p = 0.007$, Figure 1). Specifically, patients with Parkinson's disease with RBD showed higher ^{11}C-ABP688 V_T compared to HC subjects (mean difference 0.534, 95% CI 0.138 – 0.930, $p = 0.009$) and patients without RBD (mean difference 0.580, 95% CI 0.196 – 0.964, $p = 0.004$), whereas the latter two groups did not differ ($p = 0.812$). A significantly higher ^{11}C-ABP688 V_T in Parkinson's disease with RBD was observed in all cortical and subcortical brain regions compared to patients without RBD and HC subjects (Figure 2).

Group differences remained significant when all demographic and clinical metrics (age, sex, BMI, olfaction, MoCA, GDS 15, RBDSQ, PDSS, and SCOPA-AUT), and metabolite corrected plasma concentrations of ^{11}C-ABP688 were considered as covariates (overall effect: $F(2,35) = 4.787$, $p = 0.015$, Parkinson's disease with RBD versus HC: $p = 0.047$, Parkinson's disease with RBD versus Parkinson's disease without RBD; $p = 0.004$).

The comparison of glutamatergic metabolites - glutamate, glutamine, and glutathione - estimated from MR spectroscopy of the left putamen did not reveal significant differences across the three groups (Table 3). The amount of grey and white matter included in the spectroscopy voxel and the spectroscopy quality criteria were comparable across groups (Table 3). None of the estimated glutamate metabolites exhibited a significant covariation with ^{11}C-ABP688 V_T when evaluated with a repeated measures ANCOVA (all $p > 0.8$, interaction term with brain region: all $p > 0.2$). Additionally, correlation analyses of glutamate metabolites with ^{11}C-ABP688 V_T of the left putamen did not reveal significant correlations (all $|r| < 0.100$, all $p > 0.500$).

Clinical correlates of ^{11}C-ABP688 V_T

Besides a dichotomized effect of RBD status, we found a linear association between ^{11}C-ABP688 V_T of all examined brain regions and the amount of RSWA in patients with Parkinson's disease when including 'any activity' in a repeated measures ANCOVA ($F(1,27) = 4.462$, $p = 0.044$, including patients with Parkinson's disease only and $F(1,42) = 5.600$, $p = 0.023$, including all subjects in analysis).

To interrogate correlates of motor performance in patients with Parkinson's disease with ^{11}C-ABP688 V_T, we reduced the examined brain regions to critical motor centers (= caudate, putamen, pallidum, and primary motor cortex). Dopaminergic treatment response negatively covaried with ^{11}C-ABP688 V_T in a repeated measures ANCOVA ($F(1,30) = 5.823$, $p = 0.022$). This was reflected in significant correlations of dopaminergic treatment response with ^{11}C-ABP688 V_T of the examined motor regions (except caudate) (Figure 3). Motor symptom duration, Hoehn & Yahr stage, and MDS-UPDRS III did not correlate with ^{11}C-ABP688 V_T of these regions.

Discussion

Using simultaneous PET/MR imaging, we discovered higher ^{11}C-ABP688 V_T, but unchanged glutamate, glutamine, and glutathione levels in Parkinson's disease patients with RBD compared to HC subjects and patients without RBD. We additionally found a linear relationship of increased RSWA as a hallmark of RBD and ^{11}C-ABP688 V_T. Thus, glutamate signaling in Parkinson's disease patients with RBD seems to be altered at the receptor level despite normal ambient concentrations of glutamate metabolites.

Glutamatergic neurotransmission in Parkinson's disease

Most studies assessing glutamatergic neurotransmission in Parkinson's disease have focused on investigating glutamate, glutamine, or Glx (i.e., the combination of glutamate and glutamine) levels with MR spectroscopy.[38] In line with our findings, these studies typically did not find significant differences between patients with Parkinson's disease and healthy controls, even though multiple brain regions, including the substantia nigra,[39] basal ganglia,[39–43] thalamus,[44,45] and cortical regions,[46–49] were evaluated. As glutamatergic neurotransmission is determined not only by its concentration but equivalently by its receptor availability, our data confirm and extend current knowledge by simultaneously assessing glutamate metabolomics with MR spectroscopy and changes at the receptor level using ^{11}C-ABP688 PET, suggesting a dysbalance between these two glutamate signaling factors in Parkinson's disease patients with RBD.

Interestingly, the few studies that report changes in glutamate levels using MR spectroscopy linked altered glutamate levels with impaired cognition and other neuropsychiatric conditions in Parkinson's disease.[46,50,51] These conditions are also associated with RBD in Parkinson's disease.[52] As we only included patients without relevant cognitive and psychiatric co-morbidities, changes at the receptor level might be a harbinger of more profound glutamatergic dysregulation in Parkinson's disease patients with RBD.

mGluR5, NMDA receptors, and excitotoxicity

mGluR5 (as well as mGluR1) belongs to the Group I of metabotropic glutamate receptors, which are commonly expressed in the perisynaptic zone of the postsynaptic region close to ionotropic glutamate receptors like the NMDA receptor.[53,54] Upon binding of glutamate, mGluR5 activates

$G\alpha_{q/11}$ proteins, followed by activation of phospholipase C, mobilization of calcium from intracellular storages, and eventually the activation of protein kinase C (PKC).[55] Additionally, mGluR5 interacts with Homer proteins, connecting them physically to NMDA receptors. mGluR5 contributes to the postsynaptic density, a region in tight apposition to the presynaptic active zone, which is involved in organizing receptors in the synaptic cleft.[56] Activation of mGluR5 raises the probability of channel opening in NMDA receptors and augments NMDA-mediated currents in neurons.[57,58] Conversely, activation of NMDA receptors can reverse the desensitization of mGluR5 receptors.[59] Taken together, these findings indicate that mGluR5 activation augments glutamatergic effects on NMDA receptors, thereby inducing an increased probability of excitotoxicity.[60,61]

In that sense, higher mGluR5 density in Parkinson's disease patients with RBD could lead to increased activation of NMDA receptors even in the absence of elevated glutamate levels and thereby cause excessive excitatory activity and potentially augment excitotoxicity.[62] Excitotoxicity is further enhanced by glutamate release from glia cells, which also express mGluR5.[63] mGluR5 is also reported to be upregulated in reactive astrocytes.[64,65] However, reduced imidazoline 2 binding sites, a marker of reactive astrocytes, were observed in a recent PET study in mid-stage to advanced patients with Parkinson's disease compared to HC subjects and early-stage patients.[66] Hence, as we also examined mid-stage patients, it seems unlikely that the increased ^{11}C-ABP688 binding that we observed in Parkinson's disease patients with RBD is driven by upregulation of the receptor in reactive astrocytes. Instead, we suggest that this change results from dysregulation in neurons.

Notably, activation of mGluR5 can entail a neuroprotective effect in specific cell culture models depending on the stimulation paradigm.[67] However, the authors conclude that such a switch from facilitation to inhibition of excitotoxicity might more likely occur in the initial phase of an acute event (e.g., as a result of ischemia) but not in chronic neurodegenerative disorders.[67] Following this notion, excessive glutamatergic action, like the overactivation of NMDA receptors, is more likely to be linked to excitotoxicity, particularly in Parkinson's disease.[20,68]

Moreover, activation of mGluR5 aggravated 1-methyl-4-phenyl-1,2,3,6-tetrahydropyridine (MPTP)-induced nigro-striatal damage in mice.[19] Conversely, mGluR5 antagonists showed neuroprotective effects in animal models of Parkinson's disease, attenuating cell death of dopaminergic neurons of the substantia nigra and reducing microglial activation.[69,70] Inhibition of

mGluR5 in the context of MPTP lesioning also enhanced survival of dopaminergic and noradrenergic neurons in monkeys.[18]

Multiple studies demonstrated that Parkinson's disease patients with RBD have a faster motor progression and even accelerated dopamine transporter loss and more pronounced brain atrophy compared to patients without RBD, linking RBD in Parkinson's disease to a diffuse-malignant phenotype of the disease.[6,7,71–73] Our data indicating a higher mGluR5 density in Parkinson's disease patients with RBD – potentially leading to amplified excitotoxicity even in the absence of elevated glutamate levels – align with these clinical findings, which suggests a putative pathomechanism. The association between receptor changes and RBD in Parkinson's disease is strengthened by elevated RSWA, the hallmark of RBD, also being associated with ^{11}C-ABP688 binding.

Association of mGluR5 with dopaminergic treatment

Besides our finding of elevated ^{11}C-ABP688 V_T in Parkinson's disease patients with RBD, we could link these changes at the receptor level to reduced dopaminergic treatment effects, which might - in part - provide an additional explanation of a worse motor phenotype in patients with RBD. From animal studies, it is well known that mGluR5 antagonists can mitigate parkinsonian motor symptoms, emphasizing their essential role in the basal ganglia circuitry.[74] Conversely, mGluR5 activation selectively activated the indirect pathway in a Parkinson's disease rat model.[75] More generally, downstream signaling of mGluR5 is supposed to counteract dopaminergic action in the basal ganglia.[16] Hence, the negative correlation of ^{11}C-ABP688 V_T and dopaminergic treatment effects we observed in patients with Parkinson's disease fits well with the animal data.

In the past years, modern mGluR5 antagonists like mavoglurant and dipraglurant were evaluated in phase 2 studies on patients with Parkinson's disease and revealed good safety and tolerability.[76,77] However, they failed to show efficacy in reducing levodopa-induced dyskinesia[78,79] despite substantial pre-clinical data on the beneficial effects of mGluR5 antagonists on levodopa-induced dyskinesias in various animal models of Parkinson's disease.[80,81]

Our *in-vivo* data hint at a potential role of these drugs as co-medication to facilitate dopaminergic response. Furthermore, their application in Parkinson's disease patients with RBD might ameliorate the diffuse-malignant phenotype, which warrants further investigation.

Limitations

We only used a single voxel for MR spectroscopy, centred in the left putamen, to estimate concentrations of glutamate metabolites. We, therefore, cannot exclude concentration differences in other brain regions. Such differences might be detected with more advanced techniques like spectroscopic imaging and chemical exchange saturation transfer (CEST),[82] which were not used within the constraints of this study. However, we did not observe a significant correlation of the putaminal glutamate metabolites with ^{11}C-ABP688 V_T in the putamen, and it remains unlikely that global changes of ^{11}C-ABP688 V_T in Parkinson's disease with RBD are driven by locally restricted changes in concentrations of glutamate metabolites. Furthermore, MR spectroscopy provides averaged metabolite concentrations of the whole tissue in the voxel but cannot differentiate between the components. We, therefore, analyzed multiple glutamate metabolites including glutamate, glutamine, and glutathione, which are in a tightly interconnected biochemical cycle involving neurons and astroglia, to increase sensitivity to any changes.[83]

We estimated mGluR5 density by ^{11}C-ABP688 V_T, which includes free tracer, specific and non-specific binding of ^{11}C-ABP688. We did not calculate more specific non-displaceable binding potentials due to the lack of a suitable reference region for ^{11}C-ABP688 devoid of receptors.[84] However, we thoroughly assessed ^{11}C-ABP688 kinetics during the applied bolus-infusion protocol to confirm steady-state conditions for firm quantifications.[30]

We evaluated dopaminergic treatment response in a real-life scenario with quantifying ON motor performance during a regular therapeutic regime and OFF performance after 12 hours of overnight medication withdrawal. Due to ethical considerations, we did not apply sustained withdrawals of medication and standardized doses of levodopa. This might explain why the observed mean treatment response was below 30%, which is demanded by the MDS clinical diagnostic criteria.[1] However, all patients were additionally interviewed for their subjective treatment response and fulfilled the given diagnostic criteria at the clinically established and probable Parkinson's disease levels.[1]

Conclusions

Combining ^{11}C-ABP688 PET and MR spectroscopy, we revealed altered glutamate signaling, leading to a dysbalance between changes at the receptor level and glutamate metabolism in Parkinson's disease patients with RBD. These imaging findings were associated with core clinical features of patients with this malignant phenotype: an increased amount of RSWA and reduced response to dopaminergic treatment. Our data suggest a pathomechanism that might impact the Parkinson's disease phenotype providing a rationale for further investigations of drugs targeting the mGluR5 in these patients.

Authors' contributions

CEJD: Conceptualization, Methodology, Major role in data acquisition, Writing – Review & Editing. AS: Major role in data acquisition, Data processing, Writing – Review & Editing. EF: Methodology, Software, Formal analysis, Writing - Review & Editing. CRB: Methodology, Writing - Review & Editing. LH: Visualization, Writing - Review & Editing. CPF: Formal analysis, Writing - Review & Editing. AG: Methodology, Software, Formal analysis, Writing - Review & Editing. NJS: Resources, Writing - Review & Editing. CWL: Methodology, Software, Resources, Writing - Review & Editing. BN: Resources. KJL: Methodology, Resources, Writing - Review & Editing. GRF: Resources, Writing - Review & Editing, Supervision, Funding acquisition. MS: Conceptualization, Methodology, Formal analysis, Major role in data acquisition, Resources, Data curation, Writing – Original Draft, Visualization, Super vision, Project administration, Funding acquisition.

Acknowledgments

We thank all study participants and Michael Barbe for his support in patient recruitment. We highly appreciate the technical support of Lutz Tellmann and the professional patient care of Silke Frensch and Suzanne Schaden during PET/MR scanning. We would like to acknowledge E.J. Auerbach and M. Marjanska (Center for Magnetic Resonance Research and Department of Radiology, University of Minnesota, USA) for the development of the STEAM and FASTESTMAP sequences for the Siemens platform, which was provided by the University of Minnesota under a C2P agreement. We also acknowledge D. Deelchand for providing access to the macromolecular spectrum used here.

Disclosures

C. E. J. Doppler is supported by the Clinician Scientist Program (CCSP) / Faculty of Medicine / University of Cologne, funded by the Deutsche Forschungsgemeinschaft (DFG, German Research Foundation, FI 773/15-1)

A. Seger, E. Farrher, C. Régio Brambilla, L. Hensel, C. P. Filss and A. Gogishvili report no disclosures.

N. J. Shah received institutional funding's.

C. W. Lerche, B. Neumaier, and K. Langen report no disclosures.

G. R. Fink is funded by the Deutsche Forschungsgemeinschaft (DFG, German Research Foundation) – Project-ID 431549029 – SFB 1451. GRF serves as an editorial board member of Cortex, Neurological Research and Practice, NeuroImage: Clinical, Zeitschrift für Neuropsychologie, and DGNeurologie; receives royalties from the publication of the books Funktionelle MRT in Psychiatrie und Neurologie, Neurologische Differentialdiagnose, and SOP Neurologie; received honoraria for speaking engagements from Bayer, Desitin, Ergo DKV, Forum für medizinische Fortbildung FomF GmbH, GSK, Medica Academy Messe Düsseldorf, Medicbrain Healthcare, Novartis, Pfizer, and Sportärztebund NRW.

M. Sommerauer is funded by the Koeln Fortune Program / Faculty of Medicine, University of Cologne (grant number 453/2018), and the Else Kröner-Fresenius-Stiftung (grant number 2019_EKES.02).

References

1. Postuma RB, Berg D, Stern M, et al. MDS clinical diagnostic criteria for Parkinson's disease: MDS-PD Clinical Diagnostic Criteria. *Mov Disord*. 2015;30(12):1591-1601. doi:10.1002/mds.26424

2. Berg D, Borghammer P, Fereshtehnejad SM, et al. Prodromal Parkinson disease subtypes — key to understanding heterogeneity. *Nature Reviews Neurology*. Published online April 20, 2021:1-13. doi:10/gjs6zx

3. Blesa J, Foffani G, Dehay B, Bezard E, Obeso JA. Motor and non-motor circuit disturbances in early Parkinson disease: which happens first? *Nat Rev Neurosci*. 2022;23(2):115-128. doi:10.1038/s41583-021-00542-9

4. Borghammer P, Horsager J, Andersen K, et al. Neuropathological evidence of body-first vs. brain-first Lewy body disease. *Neurobiology of Disease*. 2021;161:105557. doi:10.1016/j.nbd.2021.105557

5. Horsager J, Knudsen K, Sommerauer M. Clinical and imaging evidence of brain-first and body-first Parkinson's disease. *Neurobiology of Disease*. 2022;164:105626. doi:10.1016/j.nbd.2022.105626

6. Sommerauer M, Valko PO, Werth E, Poryazova R, Hauser S, Baumann CR. Revisiting the impact of REM sleep behavior disorder on motor progression in Parkinson's disease. *Parkinsonism & Related Disorders*. 2014;20(4):460-462. doi:10.1016/j.parkreldis.2014.01.005

7. Fereshtehnejad SM, Romenets SR, Anang JBM, Latreille V, Gagnon JF, Postuma RB. New Clinical Subtypes of Parkinson Disease and Their Longitudinal Progression: A Prospective Cohort Comparison With Other Phenotypes. *JAMA Neurol*. 2015;72(8):863. doi:10.1001/jamaneurol.2015.0703

8. Sommerauer M, Fedorova TD, Hansen AK, et al. Evaluation of the noradrenergic system in Parkinson's disease: an 11C-MeNER PET and neuromelanin MRI study. *Brain*. 2018;141(2):496-504. doi:10.1093/brain/awx348

9. Kotagal V, Albin RL, Müller MLTM, et al. Symptoms of rapid eye movement sleep behavior disorder are associated with cholinergic denervation in Parkinson disease. *Ann Neurol*. 2012;71(4):560-568. doi:10.1002/ana.22691

10. Espay AJ, Morgante F, Merola A, et al. Levodopa-induced dyskinesia in Parkinson disease: Current and evolving concepts: Dyskinesia in PD. *Ann Neurol*. 2018;84(6):797-811. doi:10.1002/ana.25364

11. Nedergaard M, Takano T, Hansen AJ. Beyond the role of glutamate as a neurotransmitter. *Nat Rev Neurosci*. 2002;3(9):748-755. doi:10.1038/nrn916

12. Andersen JV, Markussen KH, Jakobsen E, et al. Glutamate metabolism and recycling at the excitatory synapse in health and neurodegeneration. *Neuropharmacology*. 2021;196:108719. doi:10.1016/j.neuropharm.2021.108719

13. Pinheiro PS, Mulle C. Presynaptic glutamate receptors: physiological functions and mechanisms of action. *Nat Rev Neurosci*. 2008;9(6):423-436. doi:10.1038/nrn2379

14. Ribeiro FM, Vieira LB, Pires RGW, Olmo RP, Ferguson SSG. Metabotropic glutamate receptors and neurodegenerative diseases. *Pharmacological Research*. 2017;115:179-191. doi:10.1016/j.phrs.2016.11.013

15. Luppi PH, Clément O, Valencia Garcia S, Brischoux F, Fort P. New aspects in the pathophysiology of rapid eye movement sleep behavior disorder: the potential role of glutamate, gamma-aminobutyric acid, and glycine. *Sleep Medicine*. 2013;14(8):714-718. doi:10.1016/j.sleep.2013.02.004

16. Conn PJ, Battaglia G, Marino MJ, Nicoletti F. Metabotropic glutamate receptors in the basal ganglia motor circuit. *Nat Rev Neurosci*. 2005;6(10):787-798. doi:10.1038/nrn1763

17. Grégoire L, Morin N, Ouattara B, et al. The acute antiparkinsonian and antidyskinetic effect of AFQ056, a novel metabotropic glutamate receptor type 5 antagonist, in l-Dopa-treated parkinsonian monkeys. *Parkinsonism & Related Disorders*. 2011;17(4):270-276. doi:10.1016/j.parkreldis.2011.01.008

18. Masilamoni GJ, Bogenpohl JW, Alagille D, et al. Metabotropic glutamate receptor 5 antagonist protects dopaminergic and noradrenergic neurons from degeneration in MPTP-treated monkeys. *Brain*. 2011;134(7):2057-2073. doi:10.1093/brain/awr137

19. Battaglia G. Endogenous Activation of mGlu5 Metabotropic Glutamate Receptors Contributes to the Development of Nigro-Striatal Damage Induced by 1-Methyl-4-Phenyl-1,2,3,6-Tetrahydropyridine in Mice. *Journal of Neuroscience*. 2004;24(4):828-835. doi:10.1523/JNEUROSCI.3831-03.2004

20. Wang J, Wang F, Mai D, Qu S. Molecular Mechanisms of Glutamate Toxicity in Parkinson's Disease. *Front Neurosci*. 2020;14:585584. doi:10.3389/fnins.2020.585584

21. Akkus F, Ametamey SM, Treyer V, et al. Marked global reduction in mGluR5 receptor binding in smokers and ex-smokers determined by [^{11} C]ABP688 positron emission tomography. *Proc Natl Acad Sci USA*. 2013;110(2):737-742. doi:10.1073/pnas.1210984110

22. Tomlinson CL, Stowe R, Patel S, Rick C, Gray R, Clarke CE. Systematic review of levodopa dose equivalency reporting in Parkinson's disease: Systematic Review of LED Reporting in PD. *Mov Disord*. 2010;25(15):2649-2653. doi:10.1002/mds.23429

23. Berry R, Quan S, Abreu A, Bibbs M, DelRosso L, Harding S. *The AASM Manual for the Scoring of Sleep and Associated Events: Rules, Terminology and Technical Specifications. Version 2.6*. American Academy of Sleep Medicine; 2020.

24. Frauscher B, Iranzo A, Gaig C, et al. Normative EMG Values during REM Sleep for the Diagnosis of REM Sleep Behavior Disorder. *Sleep*. 2012;35(6):835-847. doi:10.5665/sleep.1886

25. Elmenhorst D, Mertens K, Kroll T, et al. Circadian variation of metabotropic glutamate receptor 5 availability in the rat brain. *J Sleep Res*. 2016;25(6):754-761. doi:10.1111/jsr.12432

26. Herzog H, Langen KJ, Weirich C, et al. High resolution BrainPET combined with simultaneous MRI. *Nuklearmedizin*. 2011;50(02):74-82. doi:10.3413/Nukmed-0347-10-09

27. Burger C, Deschwanden A, Ametamey S, et al. Evaluation of a bolus/infusion protocol for 11C-ABP688, a PET tracer for mGluR5. *Nuclear Medicine and Biology*. 2010;37(7):845-851. doi:10.1016/j.nucmedbio.2010.04.107

28. Kops ER, Herzog H, Shah NJ. Comparison template-based with CT-based attenuation correction for hybrid MR/PET scanners. *EJNMMI Phys*. 2014;1(S1):A47, 2197-7364-1-S1-A47. doi:10.1186/2197-7364-1-S1-A47

29. Régio Brambilla C, Veselinović T, Rajkumar R, et al. mGluR5 binding changes during a mismatch negativity task in a multimodal protocol with [11C]ABP688 PET/MR-EEG. *Transl Psychiatry*.

2022;12(1):6. doi:10.1038/s41398-021-01763-3

30. Innis RB, Cunningham VJ, Delforge J, et al. Consensus Nomenclature for *in vivo* Imaging of Reversibly Binding Radioligands. *J Cereb Blood Flow Metab*. 2007;27(9):1533-1539. doi:10.1038/sj.jcbfm.9600493

31. Tkáč I, Star?uk Z, Choi IY, Gruetter R. In vivo^{1}H NMR spectroscopy of rat brain at 1 ms echo time. *Magn Reson Med*. 1999;41(4):649-656. doi:10.1002/(SICI)1522-2594(199904)41:4<649::AID-MRM2>3.0.CO;2-G

32. Gruetter R, Tkáč I. Field mapping without reference scan using asymmetric echo-planar techniques. *Magn Reson Med*. 2000;43(2):319-323. doi:10.1002/(SICI)1522-2594(200002)43:2<319::AID-MRM22>3.0.CO;2-1

33. Simpson R, Devenyi GA, Jezzard P, Hennessy TJ, Near J. Advanced processing and simulation of MRS data using the FID appliance (FID A)—An open source, MATLAB based toolkit. *Magn Reson Med*. 2017;77(1):23-33. doi:10.1002/mrm.26091

34. Soher BJ, Semanchuk P, Todd D, Steinberg J, Young K. VeSPA: integrated applications for RF pulse design, spectral simulation and MRS data analysis. In: *Proceedings of the International Society for Magnetic Resonance in Medicine*. Vol 19. ; 2011:1410.

35. Govindaraju V, Young K, Maudsley AA. Proton NMR chemical shifts and coupling constants for brain metabolites. *NMR Biomed*. 2000;13(3):129-153. doi:10.1002/1099-1492(200005)13:3<129::AID-NBM619>3.0.CO;2-V

36. Zhang Y, Brady M, Smith S. Segmentation of brain MR images through a hidden Markov random field model and the expectation-maximization algorithm. *IEEE Trans Med Imaging*. 2001;20(1):45-57. doi:10/b647tb

37. Patenaude B, Smith SM, Kennedy DN, Jenkinson M. A Bayesian model of shape and appearance for subcortical brain segmentation. *NeuroImage*. 2011;56(3):907-922. doi:10.1016/j.neuroimage.2011.02.046

38. Chaudhary S, Kumari S, Kumaran SS, Goyal V, Jain S, Kaloiya GS. In vitro and in vivo NMR based metabolomics in Parkinson's disease. *Journal of Magnetic Resonance Open*. 2022;10-11:100050. doi:10.1016/j.jmro.2022.100050

39. Emir UE, Tuite PJ, Öz G. Elevated Pontine and Putamenal GABA Levels in Mild-Moderate Parkinson Disease Detected by 7 Tesla Proton MRS. Rameshwar P, ed. *PLoS ONE*. 2012;7(1):e30918. doi:10.1371/journal.pone.0030918

40. Clarke CE, Lowry M, Horsman A. Unchanged basal gangliaN-acetylaspartate and glutamate in idiopathic Parkinson's disease measured by proton magnetic resonance spectroscopy. *Mov Disord*. 1997;12(3):297-301. doi:10.1002/mds.870120306

41. Clarke CE, Lowry M. Basal ganglia metabolite concentrations in idiopathic Parkinson's disease and multiple system atrophy measured by proton magnetic resonance spectroscopy. *European Journal of Neurology*. 2000;7(6):661-665. doi:10.1046/j.1468-1331.2000.00111.x

42. Kickler N, Krack P, Fraix V, et al. Glutamate measurement in Parkinson's disease using MRS at 3 T field strength. *NMR Biomed*. 2007;20(8):757-762. doi:10.1002/nbm.1141

43. Mazuel L, Chassain C, Jean B, et al. Proton MR Spectroscopy for Diagnosis and Evaluation of Treatment Efficacy in Parkinson Disease. *Radiology*. 2016;278(2):505-513. doi:10.1148/radiol.2015142764

44. Pesch B, Casjens S, Woitalla D, et al. Impairment of Motor Function Correlates with Neurometabolite and Brain Iron Alterations in Parkinson's Disease. *Cells*. 2019;8(2):96. doi:10.3390/cells8020096

45. Barbagallo G, Arabia G, Morelli M, et al. Thalamic neurometabolic alterations in tremulous Parkinson's disease: A preliminary proton MR spectroscopy study. *Parkinsonism & Related Disorders*. 2017;43:78-84. doi:10.1016/j.parkreldis.2017.07.028

46. Buard I, Lopez-Esquibel N, Carey FJ, et al. Does Prefrontal Glutamate Index Cognitive Changes in Parkinson's Disease? *Front Hum Neurosci*. 2022;16:809905. doi:10.3389/fnhum.2022.809905

47. Delli Pizzi S, Franciotti R, Ferretti A, et al. High γ□Aminobutyric Acid Content Within the Medial Prefrontal Cortex Is a Functional Signature of Somatic Symptoms Disorder in Patients With Parkinson's Disease. *Mov Disord*. 2020;35(12):2184-2192. doi:10.1002/mds.28221

48. Klietz M, Bronzlik P, Nösel P, et al. Altered Neurometabolic Profile in Early Parkinson's Disease: A Study With Short Echo-Time Whole Brain MR Spectroscopic Imaging. *Front Neurol*. 2019;10:777. doi:10.3389/fneur.2019.00777

49. O'Gorman Tuura RL, Baumann CR, Baumann-Vogel H. Beyond Dopamine: GABA, Glutamate, and the Axial Symptoms of Parkinson Disease. *Front Neurol*. 2018;9:806. doi:10.3389/fneur.2018.00806

50. Su L, Blamire AM, Watson R, He J, Hayes L, O'Brien JT. Whole-brain patterns of 1H-magnetic resonance spectroscopy imaging in Alzheimer's disease and dementia with Lewy bodies. *Transl Psychiatry*. 2016;6(8):e877-e877. doi:10.1038/tp.2016.140

51. Rodríguez-Violante M, Cervantes-Arriaga A, González-Latapí P, León-Ortiz P, de la Fuente-Sandoval C, Corona T. Proton Magnetic Resonance Spectroscopy Changes in Parkinson's Disease With and Without Psychosis. *Rev Invest Clin*. 2015;67(4):227-234.

52. Guo Y, Liu FT, Hou XH, et al. Predictors of cognitive impairment in Parkinson's disease: a systematic review and meta-analysis of prospective cohort studies. *J Neurol*. 2021;268(8):2713-2722. doi:10.1007/s00415-020-09757-9

53. Luján R, Nusser Z, Roberts JDB, Shigemoto R, Somogyi P. Perisynaptic Location of Metabotropic Glutamate Receptors mGluR1 and mGluR5 on Dendrites and Dendritic Spines in the Rat Hippocampus. *European Journal of Neuroscience*. 1996;8(7):1488-1500. doi:10.1111/j.1460-9568.1996.tb01611.x

54. Shigemoto R, Nomura S, Ohishi H, Sugihara H, Nakanishi S, Mizuno N. Immunohistochemical localization of a metabotropic glutamate receptor, mGluR5, in the rat brain. *Neuroscience Letters*. 1993;163(1):53-57. doi:10.1016/0304-3940(93)90227-C

55. Niswender CM, Conn PJ. Metabotropic Glutamate Receptors: Physiology, Pharmacology, and Disease. *Annu Rev Pharmacol Toxicol*. 2010;50(1):295-322. doi:10.1146/annurev.pharmtox.011008.145533

56. Moraes BJ, Coelho P, Fão L, Ferreira IL, Rego AC. Modified Glutamatergic Postsynapse in Neurodegenerative Disorders. *Neuroscience*. 2021;454:116-139. doi:10.1016/j.neuroscience.2019.12.002

57. Lu WY, Xiong ZG, Lei S, et al. G-protein-coupled receptors act via protein kinase C and Src to regulate NMDA receptors. *Nat Neurosci*. 1999;2(4):331-338. doi:10.1038/7243

58. Heidinger V, Manzerra P, Wang XQ, et al. Metabotropic Glutamate Receptor 1-Induced Upregulation of NMDA Receptor Current: Mediation through the Pyk2/Src-Family Kinase Pathway in Cortical Neurons. *J Neurosci*. 2002;22(13):5452-5461. doi:10.1523/JNEUROSCI.22-13-05452.2002

59. Alagarsamy S, Marino MJ, Rouse ST, Gereau RW, Heinemann SF, Conn PJ. Activation of NMDA receptors reverses desensitization of mGluR5 in native and recombinant systems. *Nat Neurosci*. 1999;2(3):234-240. doi:10.1038/6338

60. Hilton GD, Nunez JL, Bambrick L, Thompson SM, McCarthy MM. Glutamate-mediated excitotoxicity in neonatal hippocampal neurons is mediated by mGluR-induced release of Ca^{++} from intracellular stores and is prevented by estradiol. *European Journal of Neuroscience*. 2006;24(11):3008-3016. doi:10.1111/j.1460-9568.2006.05189.x

61. Tsai VWW, Scott HL, Lewis RJ, Dodd PR. The role of group I metabotropic glutamate receptors in neuronal excitotoxicity in alzheimer's disease. *neurotox res*. 2005;7(1-2):125-141. doi:10.1007/BF03033782

62. Calabresi P, Centonze D, Pisani A, Bernardi G. Metabotropic Glutamate Receptors and Cell-Type-Specific Vulnerability in the Striatum: Implication for Ischemia and Huntington's Disease. *Experimental Neurology*. 1999;158(1):97-108. doi:10.1006/exnr.1999.7092

63. Pasti L, Volterra A, Pozzan T, Carmignoto G. Intracellular Calcium Oscillations in Astrocytes: A Highly Plastic, Bidirectional Form of Communication between Neurons and Astrocytes *In Situ*. *J Neurosci*. 1997;17(20):7817-7830. doi:10.1523/JNEUROSCI.17-20-07817.1997

64. Aronica E, Van Vliet EA, Mayboroda OA, Troost D, Da Silva FHL, Gorter JA. Upregulation of metabotropic glutamate receptor subtype mGluR3 and mGluR5 in reactive astrocytes in a rat model of mesial temporal lobe epilepsy: mGluR expression in reactive astrocytes of epileptic rats. *European Journal of Neuroscience*. 2000;12(7):2333-2344. doi:10.1046/j.1460-9568.2000.00131.x

65. Ferraguti F, Corti C, Valerio E, Mion S, Xuereb J. Activated astrocytes in areas of kainate-induced neuronal injury upregulate the expression of the metabotropic glutamate receptors 2/3 and 5. *Experimental Brain Research*. 2001;137(1):1-11. doi:10.1007/s002210000633

66. Wilson H, Dervenoulas G, Pagano G, et al. Imidazoline 2 binding sites reflecting astroglia pathology in Parkinson's disease: an in vivo11C-BU99008 PET study. *Brain*. 2019;142(10):3116-3128. doi:10.1093/brain/awz260

67. Bruno V, Battaglia G, Copani A, et al. An activity-dependent switch from facilitation to inhibition in the control of excitotoxicity by group I metabotropic glutamate receptors: Functional switch of group I mGluRs in neurodegeneration. *European Journal of Neuroscience*. 2001;13(8):1469-1478. doi:10.1046/j.0953-816x.2001.01541.x

68. Lynch DR, Guttmann RP. Excitotoxicity: Perspectives Based on *N* -Methyl-d-Aspartate Receptor Subtypes. *J Pharmacol Exp Ther*. 2002;300(3):717-723. doi:10.1124/jpet.300.3.717

69. Chen L, Liu J, Ali U, et al. Chronic, systemic treatment with a metabotropic glutamate receptor 5 antagonist produces anxiolytic-like effects and reverses abnormal firing activity of projection neurons in the basolateral nucleus of the amygdala in rats with bilateral 6-OHDA lesions. *Brain Research Bulletin*.

2011;84(3):215-223. doi:10.1016/j.brainresbull.2011.01.005

70. Hsieh MH, Ho SC, Yeh KY, et al. Blockade of metabotropic glutamate receptors inhibits cognition and neurodegeneration in an MPTP-induced Parkinson's disease rat model. *Pharmacology Biochemistry and Behavior*. 2012;102(1):64-71. doi:10.1016/j.pbb.2012.03.022

71. Pagano G, De Micco R, Yousaf T, Wilson H, Chandra A, Politis M. REM behavior disorder predicts motor progression and cognitive decline in Parkinson disease. *Neurology*. 2018;91(10):e894-e905. doi:10.1212/WNL.0000000000006134

72. Rahayel S, Gaubert M, Postuma RB, et al. Brain atrophy in Parkinson's disease with polysomnography-confirmed REM sleep behavior disorder. *Sleep*. 2019;42(6):zsz062. doi:10/gmnvr7

73. Yoon EJ, Monchi O. Probable REM sleep behavior disorder is associated with longitudinal cortical thinning in Parkinson's disease. *npj Parkinsons Dis*. 2021;7(1):19. doi:10.1038/s41531-021-00164-z

74. Breysse N, Baunez C, Spooren W, Gasparini F, Amalric M. Chronic But Not Acute Treatment with a Metabotropic Glutamate 5 Receptor Antagonist Reverses the Akinetic Deficits in a Rat Model of Parkinsonism. *J Neurosci*. 2002;22(13):5669-5678. doi:10.1523/JNEUROSCI.22-13-05669.2002

75. Kearney JAF, Frey KA, Albin RL. Metabotropic Glutamate Agonist-Induced Rotation: A Pharmacological, FOS Immunohistochemical, and [^{14} C]-2-Deoxyglucose Autoradiographic Study. *J Neurosci*. 1997;17(11):4415-4425. doi:10.1523/JNEUROSCI.17-11-04415.1997

76. Tison F, Keywood C, Wakefield M, et al. A Phase 2A Trial of the Novel mGluR5-Negative Allosteric Modulator Dipraglurant for Levodopa-Induced Dyskinesia in Parkinson's Disease: Dipraglurant in Levodopa-Induced Dyskinesia. *Mov Disord*. 2016;31(9):1373-1380. doi:10.1002/mds.26659

77. Trenkwalder C, Stocchi F, Poewe W, et al. Mavoglurant in Parkinson's patients with l-Dopa-induced dyskinesias: Two randomized phase 2 studies: Mavoglurant in PD Patients with LID. *Mov Disord*. 2016;31(7):1054-1058. doi:10.1002/mds.26585

78. Negida A, Ghaith HS, Fala SY, et al. Mavoglurant (AFQ056) for the treatment of levodopa-induced dyskinesia in patients with Parkinson's disease: a meta-analysis. *Neurol Sci*. 2021;42(8):3135-3143. doi:10.1007/s10072-021-05319-7

79. Wang WW, Zhang XR, Zhang ZR, et al. Effects of mGluR5 Antagonists on Parkinson's Patients With L-Dopa-Induced Dyskinesia: A Systematic Review and Meta-Analysis of Randomized Controlled Trials. *Front Aging Neurosci*. 2018;10:262. doi:10.3389/fnagi.2018.00262

80. Pourmirbabaei S, Dolatshahi M, Rahmani F. Pathophysiological clues to therapeutic applications of glutamate mGlu5 receptor antagonists in levodopa-induced dyskinesia. *European Journal of Pharmacology*. 2019;855:149-159. doi:10.1016/j.ejphar.2019.05.004

81. Sebastianutto I, Cenci MA. mGlu receptors in the treatment of Parkinson's disease and L-DOPA-induced dyskinesia. *Current Opinion in Pharmacology*. 2018;38:81-89. doi:10.1016/j.coph.2018.03.003

82. Wu B, Warnock G, Zaiss M, et al. An overview of CEST MRI for non-MR physicists. *EJNMMI Phys*. 2016;3(1):19. doi:10.1186/s40658-016-0155-2

83. O'Gorman Tuura R, Warnock G, Ametamey S, et al. Imaging glutamate redistribution after acute N-acetylcysteine administration: A simultaneous PET/MR study. *NeuroImage*. 2019;184:826-833.

doi:10.1016/j.neuroimage.2018.10.017

84. Treyer V, Streffer J, Wyss MT, et al. Evaluation of the Metabotropic Glutamate Receptor Subtype 5 Using PET and 11C-ABP688: Assessment of Methods. *Journal of Nuclear Medicine*. 2007;48(7):1207-1215. doi:10.2967/jnumed.107.039578

Table 1 Demographic and clinical characteristics

	HC	PD-RBD	PD+RBD	*p* Value
No. of participants	15	17	16	
Age [y]	66.6 ± 7.6	65.4 ± 7.4	68.1 ± 7.5	0.577*
Sex [% male]	73.3	76.5	75.0	0.979§
BMI [kg/m²]	25.4 ± 3.0	27.7 ± 4.4	26.3 ± 4.8	0.296*
Sniffin' Sticks [correct items]	9.7 ± 1.5	5.9 ± 2.5	4.3 ± 2.1	**<0.001#,1,2**
MoCA	26.7 ± 1.5	27.1 ± 1.5	26.6 ± 2.3	0.734*
GDS 15	0.7 ± 0.8	1.1 ± 1.3	1.1 ± 1.2	0.778#
RBDSQ	1.4 ± 1.7	2.9 ± 2.1	5.8 ± 2.9	**<0.001#,1,2,3**
PDSS	6.3 ± 4.9	14.8 ± 10.1	15.1 ± 9.1	**0.012#,1,2**
SCOPA-AUT	5.0 ± 3.8	10.6 ± 7.6	12.2 ± 4.9	**0.003#,1,2**
Motor symptom duration [y]		4.8 ± 2.0	6.4 ± 3.8	0.165#
Hoehn & Yahr stage		2.3 ± 0.7	2.2 ± 0.7	0.901#
MDS-UPDRS III, OFF		36.8 ± 15.3	35.3 ± 14.1	0.769*
MDS-UPDRS III, ON		26.5 ± 12.1	26.6 ± 10.5	0.982*
Treatment response [%]		28.9 ± 14.6	21.4 ± 18.5	0.218*
LEDD [mg]		490.8 ± 298.9	621.2 ± 474.1	0.488#

Abbreviations: BMI = body mass index, GDS = Geriatric Depression Scale, HC = healthy control, kg = kilograms, LEDD = levodopa equivalent daily dose, m = meters, MDS-UPDRS = Movement Disorder Society unified Parkinson's disease rating scale, mg = milligrams, MoCA = Montreal cognitive assessment, PD = Parkinson's disease, PDSS = Parkinson's disease sleep scale, RBD = REM sleep behavior disorder, RBDSQ = REM sleep behavior disorder screening questionnaire, SCOPA-AUT = scales for outcomes in Parkinson's disease - autonomic dysfunction, y = years

Statistics: * = parametric test (analysis of variance, ANOVA or Student's t-test), § = chi-square test, # = non-parametric test (Kruskal-Wallis test or Mann-Whitney U test); post-hoc test differences at $P < 0.05$ uncorrected: 1 = HC versus PD-RBD, 2 = HC versus PD+RBD, 3 = PD-RBD versus PD+RBD

Table 2 Polysomnographic metrics

	HC *n* = 15	**PD-RBD** *n* = 17	**PD+RBD** *n* = 16	*p Value*
Sleep period [min]	473.1 ± 55.2	449.2 ± 74.3	455.6 ± 68.4	0.609[*]
Sleep efficiency [%]	77.4 ± 15.6	76.5 ± 21.4	84.1 ± 11.4	0.428[#]
N1 [min]	72.9 ± 47.9	62.5 ± 30.3	62.1 ± 26.8	0.905[#]
N2 [min]	173.0 ± 49.9	183.5 ± 88.9	192.2 ± 51.0	0.727[*]
SWS [min]	59.0 ± 28.1	51.0 ± 34.8	53.3 ± 40.5	0.807[*]
REM [min]	58.1 ± 29.9	48.3 ± 32.0	73.8 ± 42.0	0.122[*]
AHI [/h]	12.4 ± 14.1	14.5 ± 13.9	10.8 ± 11.9	0.794[#]
PLMSI [/h]	29.0 ± 39.2	37.2 ± 47.7	26.5 ± 28.2	0.817[#]
RSWA, tonic [%]	0.5 ± 1.1	0.0 ± 0.0	11.2 ± 10.5	**<0.001**[#,2,3]
RSWA, phasic [%]	4.8 ± 3.3	4.9 ± 3.0	24.6 ± 9.6	**<0.001**[#,2,3]
RSWA, any [%]	5.2 ± 4.1	5.0 ± 3.1	35.1 ± 15.5	**<0.001**[#,2,3]

Abbreviations: AHI = apnea-hypopnea index, h = hour, HC = healthy control, min = minutes, N1 = non-rapid eye movement sleep stage 1, N2 = non-rapid eye movement sleep stage 2, PD = Parkinson's disease, PLMSI = periodic leg movements during sleep index, RBD = REM sleep behavior disorder, REM = rapid eye movement sleep stage, RSWA = rapid eye movement sleep without atonia, SWS = slow-wave sleep

Statistics: [*] = parametric test (analysis of variance, ANOVA), [#] = non-parametric test (Kruskal-Wallis test); post-hoc test differences at $P < 0.05$ uncorrected: [1] = HC versus PD-RBD, [2] = HC versus PD+RBD, [3] = PD-RBD versus PD+RBD

Table 3 Magnetic resonance spectroscopy estimates of glutamatergic metabolism

	HC *n* = 11	**PD-RBD** *n* = 13	**PD+RBD** *n* = 11	*p Value*
Fraction GM	0.59 ± 0.05	0.59 ± 0.03	0.59 ± 0.03	0.781[#]
Fraction WM	0.39 ± 0.05	0.39 ± 0.03	0.38 ± 0.03	0.879[#]
FWHM [ppm]	0.05 ± 0.01	0.05 ± 0.00	0.05 ± 0.01	0.303[#]
SNR	30.9 ± 3.6	29.2 ± 3.2	29.1 ± 5.1	0.481[*]
Glutamate [mM]	5.8 ± 0.6	5.9 ± 0.4	5.6 ± 0.5	0.527[*]
CRLB [%]	4.2 ± 0.6	4.4 ± 0.7	4.6 ± 0.5	0.371[#]
Glutamine [mM]	2.9 ± 0.3	3.0 ± 0.4	2.9 ± 0.3	0.380[*]
CRLB [%]	8.6 ± 1.3	8.4 ± 1.8	9.1 ± 1.0	0.240[#]
Glutamate + Glutamine [mM]	8.6 ± 0.9	8.9 ± 0.8	8.5 ± 0.7	0.398[*]
CRLB [%]	4.0 ± 0.6	4.0 ± 0.6	4.3 ± 0.6	0.463[#]
Glutathione [mM]	0.9 ± 0.1	0.9 ± 0.1	0.8 ± 0.1	0.370[*]
CRLB [%]	10.0 ± 1.4	11.3 ± 2.5	11.6 ± 2.2	0.219[*]

Abbreviations: CRLB = Cramér–Rao lower bounds, FWHM = full width at half maximum, GM = grey matter, HC = healthy control, mM = milli molar, PD = Parkinson's disease, ppm = part per million, RBD = REM sleep behavior disorder, SNR = signal-to-noise ratio, WM = white matter

Statistics: * = parametric test (analysis of variance, ANOVA), # = non-parametric test (Kruskal-Wallis test)

Figure legends

Figure 1: ^{11}C-ABP688 volumes of distribution (V_T) images across groups. The top row shows mean V_T images sections of healthy control (HC) subjects at different levels, the middle row mean images of patients with Parkinson's disease without REM sleep behavior disorder (PD-RBD), and the bottom row mean images of patients with Parkinson's disease with REM sleep behavior disorder (PD+RBD). ^{11}C-ABP688 V_T images are scaled from 1 to 4.5 ml/cm³.

Figure 2: Regional ^{11}C-ABP688 volumes of distribution (V_T) across groups. Boxplots indicate median and upper and lower quartiles; dots represent individual data. Significant differences between groups from *post-hoc* tests of repeated measures ANOVA are indicated by asterisks (*: $p < 0.05$, **: $p < 0.01$, uncorrected). V_T is given in ml/cm³.

Abbreviations: FC = frontal cortex, TC = temporal cortex, PC = parietal cortex, OC = occipital cortex, Ins = insula, ACC = anterior cingulate, PCC = posterior cingulate, Amy = amygdala, Hip = hippocampus, Cau = caudate, Put = putamen, Pal = pallidum, and Tha = thalamus. HC = healthy control, PD-RBD = Parkinson's disease without RBD, PD+RBD = Parkinson's disease with RBD.

Figure 3: Correlation of ^{11}C-ABP688 volumes of distribution (V_T) with dopaminergic treatment response. Patients with Parkinson's disease without REM sleep behavior disorder (PD-RBD) are indicated as blue dots and patients with Parkinson's disease with REM sleep behavior disorder (PD+RBD) in purple. Pearson correlation coefficients and p-values were calculated across all patients. V_T is given in ml/cm³.

HC

PD-RBD

PD+RBD

4.5

^{11}C-ABP688 V_T

1

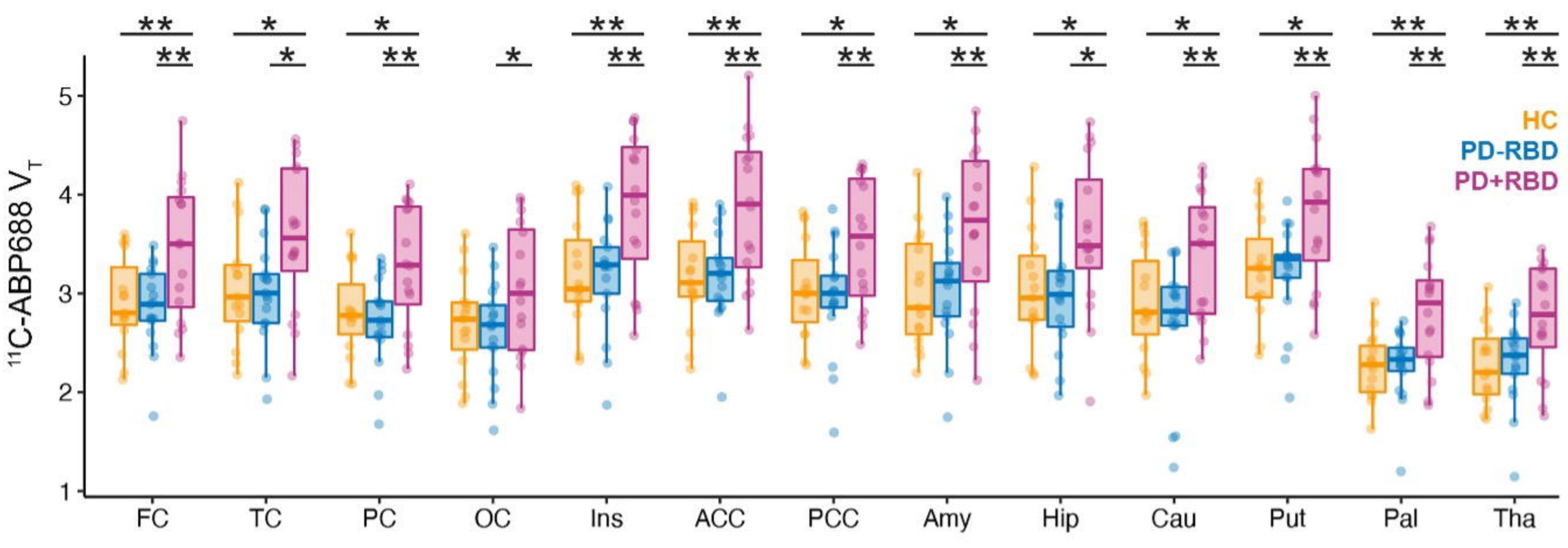
**
**
*
**
*
*
**
**
**
**
*
**
*
**
*
*
*
**
**
**
**
**
**
**
**
HC
PD-RBD
PD+RBD
^{11}C-ABP688 V_T
5
4
3
2
1
FC
TC
PC
OC
Ins
ACC
PCC
Amy
Hip
Cau
Put
Pal
Tha

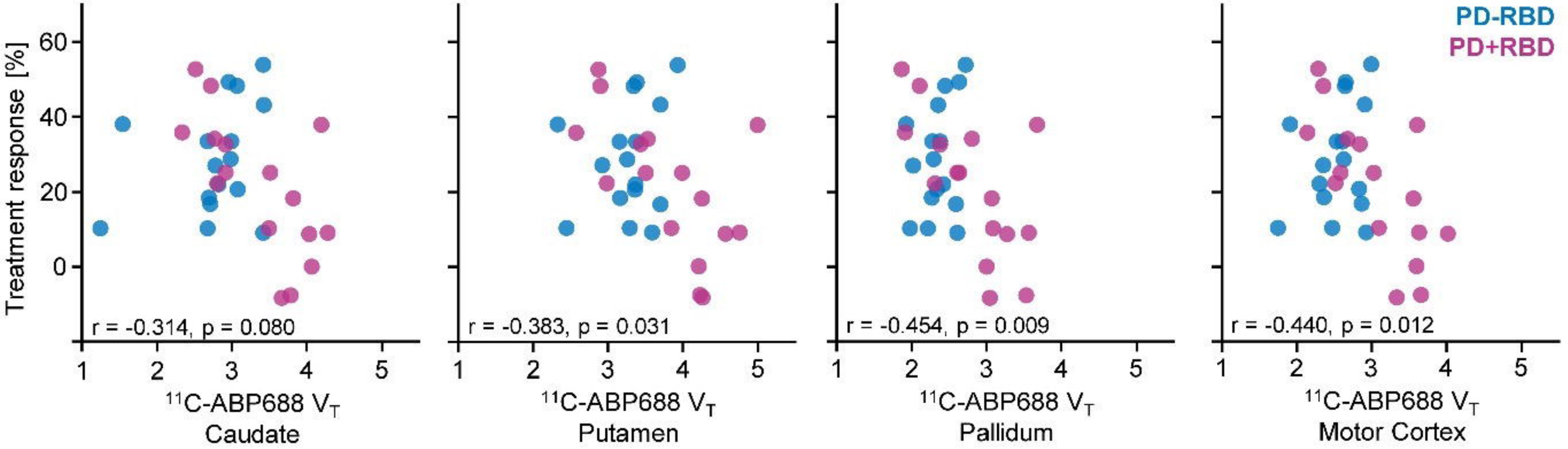
PD-RBD
PD+RBD
Treatment response [%]
60
40
20
0
r = -0.314, p = 0.080
r = -0.383, p = 0.031
r = -0.454, p = 0.009
r = -0.440, p = 0.012
1
2
3
4
5
11C-ABP688 VT
Caudate
11C-ABP688 VT
Putamen
11C-ABP688 VT
Pallidum
11C-ABP688 VT
Motor Cortex